Research Article

MRI Guided Brain Stimulation without the Use of a Neuronavigation System

Ehsan Vaghefi,[1] Peng Cai,[2] Fang Fang,[2] Winston D. Byblow,[3] Cathy M. Stinear,[4] and Benjamin Thompson[1,5]

[1] *Department of Optometry and Vision Science, University of Auckland, Building 502, Level 4, 85 Park Road, Grafton, Auckland 1023, New Zealand*
[2] *Department of Psychology, Peking University, Haidian Road, Haidian, Beijing 100871, China*
[3] *Department of Sport and Exercise Science, University of Auckland, Symonds Street, Auckland 1023, New Zealand*
[4] *Department of Medicine, University of Auckland, Symonds Street, Auckland 1023, New Zealand*
[5] *School of Optometry and Vision Science, University of Waterloo, 200 Columbia Street W, Waterloo, ON, Canada N2L 3G1*

Correspondence should be addressed to Ehsan Vaghefi; e.vaghefi@auckland.ac.nz

Received 23 June 2014; Revised 13 August 2014; Accepted 9 September 2014

Academic Editor: Zhengchao Dong

A key issue in the field of noninvasive brain stimulation (NIBS) is the accurate localization of scalp positions that correspond to targeted cortical areas. The current gold standard is to combine structural and functional brain imaging with a commercially available "neuronavigation" system. However, neuronavigation systems are not commonplace outside of specialized research environments. Here we describe a technique that allows for the use of participant-specific functional and structural MRI data to guide NIBS without a neuronavigation system. Surface mesh representations of the head were generated using Brain Voyager and vectors linking key anatomical landmarks were drawn on the mesh. Our technique was then used to calculate the precise distances on the scalp corresponding to these vectors. These calculations were verified using actual measurements of the head and the technique was used to identify a scalp position corresponding to a brain area localized using functional MRI.

1. Introduction

Noninvasive brain stimulation (NIBS) techniques such as repetitive transcranial magnetic stimulation (rTMS) and transcranial direct current stimulation (tDCS) allow for the temporary modulation of neural activity within the human brain. rTMS involves the induction of weak electrical currents within targeted regions of the cortex via brief, time-varying magnetic fields produced with a hand-held coil [1]. tDCS employs head-mounted electrodes, which allow for a weak direct current to interact with the underlying cortex [2]. NIBS can be used to investigate the role of individual brain areas in specific cognitive, behavioral, or perceptual processl [illegible] that evokes the strongest MEP can then be used as the location for rTMS or tDCS. A comparable technique also exists for the visual cortex whereby single pulse TMS of the occipital pole can be used to evoke the percept of a phosphene [8]. The scalp location that induces the most robust phosphene or a phosphene in a specific visual field location can be used for visual cortex stimulation. A similar technique can be used for motion sensitive, extra-striate visual area V5 whereby TMS can be used to induce moving phosphenes [9]. It has been shown that this technique is in good agreement with localization of V5 using functional magnetic resonance imaging [10]. However, it is not possible to use this approach outside of the motor and visual cortices because most brain regions do not produce acute neurophysiological or perceptual effects in response to single pulse TMS.

An alternative technique for identifying participant-specific stimulation sites on the scalp is the 10–20-electrode system, which was originally designed for positioning EEG electrodes [11]. This approach defines a grid of positions on the scalp that are separated by 10% or 20% of the distance between anatomical landmarks such as the nasion and the inion. This approach has been used successfully in a large number of brain stimulation studies; however, the mapping of particular 10–20 system locations to specific brain areas can vary across participants [12].

Another alternative is to use structural and functional brain imaging techniques to localize specific brain areas in individuals with millimetre resolution. A number of frameless stereotactic navigation systems exist for real-time coregistration of a participant to their own MRI images. Tools such as a "pointer" or a TMS coil can also be registered within the volume. These systems typically involve ultrasound devices or infrared cameras and a number of reference targets mounted on the head and NIBS apparatus. When used in combination with structural and functional MRI images these "neuronavigation" systems allow for precise identification of the scalp position corresponding to a particular brain area [13].

The combination of brain imaging and a neuronavigation system is the current gold standard in the field of NIBS [14] and may improve the results of NIBS-based therapeutic interventions [15–20]; however, there are some disadvantages. These include difficulty in using these systems for studies of posterior brain areas that can fall outside of the neuronavigation system's field of view and, most importantly, the high cost of these systems, which can exceed $50,000. Techniques have been described that allow NIBS to be targeted using generic MRI datasets [21

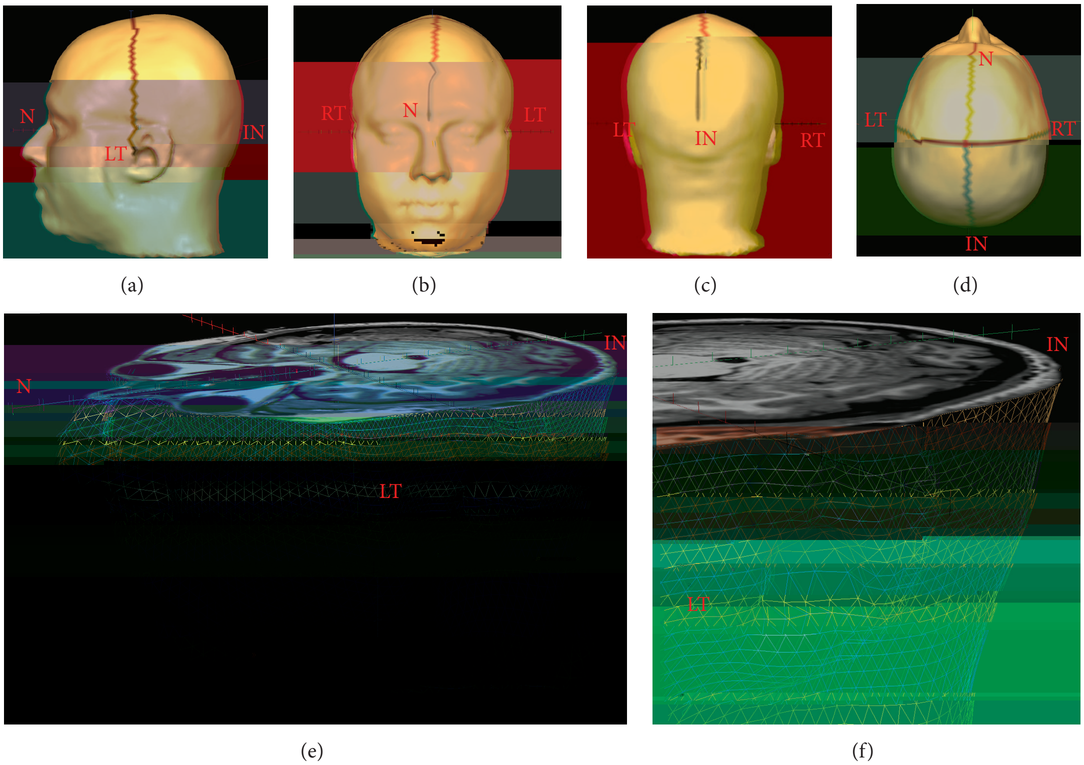

Figure 1: A 3D mesh morphed to the structural MRI data of a representative participant. Panels (a)–(d) show the anatomical landmarks that were used as anchor points for scalp distance calculations marked on a T1-volume surface mesh created using Brain Voyager. N: nasion, RT and LT: right and left tragi, respectively, and IN: inion. The lines connecting the anatomical landmarks are "patches of interest" (POIs) drawn in Brain Voyager that link adjacent triangles in the mesh. Panels (e) and (f) show close-up views of the mesh without the surface coloring. The mesh has been cut axially at the level of the inion. The smooth surface of the head is represented using triangular elements and each of these elements is defined by its tricorners.

subroutines within Brain Voyager. A general linear analysis was conducted and the results were visualized as t-maps on the anatomical image. Area V5 was identified as a region in the appropriate anatomical location that responded significantly more strongly to dynamic than static grating stimuli (FDR corrected $q < 0.01$). The precise location of V5 was defined as the location of the peak voxel within the V5 region.

2.3. Comparison of Measurements Made on the Surface Mesh and the Head. Four anatomical landmarks were identified on each surface mesh: the nasion, the left and right tragi, and the inion (Figures 1(a)–1(d)). The shortest paths between the nasion and inion and the left and right tragi that passed through the center point of the head (Cz) were then marked on the surface of the 3D mesh and exported as "patches of interest" (POIs) within Brain Voyager. After this, the x, y, and z coordinates oe the mesh nodes that formed the POI were exported from Brain Voyager in XLS format and read into the MATLAB analysis environment for distance calculations. The actual distances between the two tragi and the nasion and inion were also measured for each participant using a tape measure. An investigator masked to the results of the MATLAB analysis made these measurements.

2.4. MATLAB Operations. A Graphical User Interface was created in MATLAB to import the coordinate matrix of the POI exported from the Brain Voyager environment. Since the aim was to develop a widely applicable tool, the software does not require the use of Brian Voyager. Rather, the software is capable of reading a coordinate matrix from a text/MS-Excel file as this format is an export option in most image postprocessing software packages. The file must have three columns (x, y, z), which conform to the following format:

$$\text{Nodal}_{\text{vector}} = \left(\text{Node}\,(n)_x, \text{Node}\,(n)_y, \text{Node}\,(n)_z\right). \quad (1)$$

Here, n is the index of the nodal coordinate in the vector matrix. Subscripts x, y, and z indicate the Cartesian tricoordinates of the vector's nodal points.

The MATLAB code opens the text-based input file and searches for the first line of the nodal coordinate series. Next, it reads consecutive coordinates until the pattern is broken; that is, no further coordinates are listed. The nodes of the POI/vector can then be viewed immediately in 3D (Figure 2).

There are two main issues to be addressed when calculating scalp distances from POIs measured on a surface mesh. (1) The majority of packages that provide surface meshes (Brain Voyager included) export POIs across the mesh in a proprietary format that makes it difficult to identify adjacent

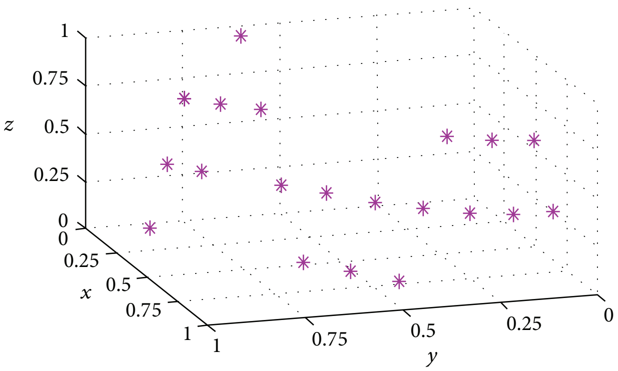

(a)

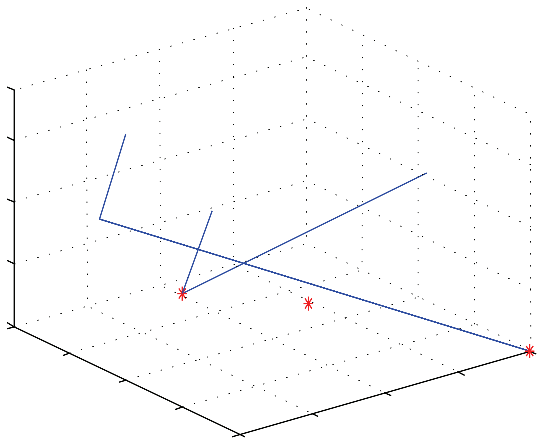


XLS File Read
Add to the Plot
Clear Plot
Vector length = 0
1
0.9
0.8
0.7
0.6
0.5
0.4
0.3
0.2
0.1
0
0 0.1 0.2 0.3 0.4 0.5 0.6 0.7 0.8 0.9 1
XLS File Read
Add to the Plot
Clear Plot
Coordinate positions of exported markers
z
x
y

(a)

[18] A. Datta, M. Bikson, and F. Fregni, "Transcranial direct current stimulation in patients with skull defects and skull plates: high-resolution computational FEM study of factors altering cortical current flow," *NeuroImage*, vol. 52, no. 4, pp. 1268–1278, 2010.

[19] F. Fregni and A. Pascual-Leone, "Technology insight: non-invasive brain stimulation in neurology—perspectives on the therapeutic potential of rTMS and tDCS," *Nature Clinical Practice Neurology*, vol. 3, no. 7, pp. 383–393, 2007.

[20] P. C. Miranda, P. Faria, and M. Hallett, "What does the ratio of injected current to electrode area tell us about current density in the brain during tDCS?" *Clinical Neurophysiology*, vol. 120, no. 6, pp. 1183–1187, 2009.

[21] F. Carducci and R. Brusco, "Accuracy of an individualized MR-based head model for navigated brain stimulation," *Psychiatry Research: Neuroimaging*, vol. 203, no. 1, pp. 105–108, 2012.

[22] F. Duecker, M. A. Frost, T. A. de Graaf et al., "The cortex-based alignment approach to TMS coil positioning," *Journal of Cognitive Neuroscience*, vol. 26, no. 10, pp. 2321–2329, 2014.

[23] P. M. Rusjan, M. S. Barr, F. Farzan et al., "Optimal transcranial magnetic stimulation coil placement for targeting the dorsolateral prefrontal cortex using novel magnetic resonance image-guided neuronavigation," *Human Brain Mapping*, vol. 31, no. 11, pp. 1643–1652, 2010.

[24] B. Thompson and Z. Liu, "Learning motion discrimination with suppressed and un-suppressed MT," *Vision Research*, vol. 46, no. 13, pp. 2110–2121, 2006.

[25] M. Nitsche, R. M. Hermann, H. Christiansen, J. Berger, and O. Pradier, "Rationale for individualized therapy in sinonasal teratocarcinosarcoma (SNTC): case report," *Onkologie*, vol. 28, no. 12, pp. 653–656, 2005.

[26] T. Morioka, T. Yamamoto, A. Mizushima et al., "Comparison of magnetoencephalography, functional MRI, and motor evoked potentials in the localization of the sensory-motor cortex," *Neurological Research*, vol. 17, no. 5, pp. 361–367, 1995.

[27] E. M. Wassermann, B. Wang, T. A. Zeffiro et al., "Locating the motor cortex on the MRI with transcranial magnetic stimulation and PET," *NeuroImage*, vol. 3, no. 1, pp. 1–9, 1996.

[28] Y. Terao, Y. Ugawa, K. Sakai et al., "Localizing the site of magnetic brain stimulation by functional MRI," *Experimental Brain Research*, vol. 121, no. 2, pp. 145–152, 1998.

[29] M.-L. Paillère Martinot, A. Galinowski, D. Ringuenet et al., "Influence of prefrontal target region on the efficacy of repetitive transcranial magnetic stimulation in patients with medication-resistant depression: a [18F]-fluorodeoxyglucose PET and MRI study," *International Journal of Neuropsychopharmacology*, vol. 13, no. 1, pp. 45–59, 2010.

[30] J. Andoh, E. Artiges, C. Pallier et al., "Modulation of language areas with functional MR image-guided magnetic stimulation," *NeuroImage*, vol. 29, no. 2, pp. 619–627, 2006.

[31] C. Rynn, C. M. Wilkinson, and H. L. Peters, "Prediction of nasal morphology from the skull," *Forensic Science, Medicine, and Pathology*, vol. 6, no. 1, pp. 20–34, 2010.

[32] A. S. Dubarry, J. M. Badier, A. Trébuchon-da Fonseca et al., "Simultaneous recording of MEG, EEG and intracerebral EEG during visual stimulation: from feasibility to single-trial analysis," *NeuroImage*, vol. 99, pp. 548–558, 2014.

[33] Z.-D. Deng, S. H. Lisanby, and A. V. Peterchev, "Electric field strength and focality in electroconvulsive therapy and magnetic seizure therapy: a finite element simulation study," *Journal of Neural Engineering*, vol. 8, no. 1, Article ID 016007, 2011.

[34] M. Bikson and A. Datta, "Guidelines for precise and accurate computational models of tDCS," *Brain Stimulation*, vol. 5, no. 3, pp. 430–431, 2012.

[35] M. Bikson, A. Rahman, A. Datta, F. Fregni, and L. Merabet, "High-resolution modeling assisted design of customized and individualized transcranial direct current stimulation protocols," *Neuromodulation*, vol. 15, no. 4, pp. 306–314, 2012.